We are IntechOpen, the world's leading publisher of Open Access books Built by scientists, for scientists

6,900
Open access books available

186,000
International authors and editors

200M
Downloads

154
Countries delivered to

Our authors are among the

TOP 1%
most cited scientists

12.2%
Contributors from top 500 universities

CLARIVATE ANALYTICS
BOOK CITATION INDEX
INDEXED

WEB OF SCIENCE™

Selection of our books indexed in the Book Citation Index
in Web of Science™ Core Collection (BKCI)

Interested in publishing with us?
Contact book.department@intechopen.com

Electrochemical, Thermodynamic, Surface, and Spectroscopic Study in Inhibition of Iron Corrosion with Turmeric Root Extract (TRE)

Khuloud Almzarzie, Ayman Almassri, Ahmad Falah and Hassan Kellawi

Abstract

Turmeric root extract was tested as corrosion inhibitor for iron in 0.5 M HCl, using potentiodynamic polarization and electrochemical impedance spectroscopy, scanning electron microscope, and energy dispersive X-ray analysis. The inhibition efficiency increases as the time of immersion rises but decreases with temperature rise. The Nyquist plots showed that the charge transfer resistance increases and the double-layer capacitance decreases as the time of immersion increases. Tafel results show that both corrosion current and corrosion speed are reduced with time of immersion. All impedance spectra of EIS tests exhibit one capacitive loop, which indicates that the corrosion reaction is controlled by charge transfer process. Inhibition efficiency increases with the concentration of the inhibitor reaching its maximum value, 88.90%, at 8 g/100 mL. Thermodynamic parameters, Ea, ΔH^*, and ΔS^*, were estimated, and the mechanism of corrosion and inhibition was discussed. The adsorption of turmeric root extract followed Langmuir adsorption isotherm.

Keywords: iron corrosion, electrochemical impedance spectroscopy (EIS), turmeric toot extract (TRE), double-layer capacitance (C_{dl}), scanning electron microscopy (SEM), inhibition efficiency IE (%)

1. Introduction

Inhibition of corrosion of iron is important for theoretical and practical aspects [1]. Iron and its alloys are of great importance in the industry, prompting vast research on corrosion resistance and its conducts [2]. Acids are wildly used in industries [3], such as industrial acid cleaning, acid descaling, and acid picking, and used to remove mill scale from metallic surfaces. Natural compounds containing sulfur, oxygen, and nitrogen atoms are effective as corrosion inhibitors in acid media; inhibitors are used to reduce the rate of dissolution of metals [4]. Natural plant inhibitors that contain organic compounds are widely used to inhibit minerals in an acidic medium [5] and are called environmentally friendly nontoxic inhibitors [6]. The adsorption of these compounds is influenced by the electronic structure of their content of active compounds, electrons density, aromatic rings, and functional

groups possessing free electrons such as, R–OH –CHO, –N=N, etc. [7]. The adsorption of organic inhibitors at the metal/solution interface takes place through the replacement of water molecules by organic inhibitor molecules [8]. The efficiency of these compounds depends mainly on their abilities to be adsorbed on the metal surface with their polar groups moving as the reactive centers. The purpose of this research is to use a nontoxic environment friendly inhibitor formed from turmeric root extract to reduce iron corrosion and study its effect using electrochemical impedance and Tafel polarization methods. Turmeric root extract contains active substances represented by turmeric derivatives with a high percentage (90%), which are phenolic compounds of antioxidant. The most important are curcumin, demethoxycurcumin, and bisdemethoxycurcumin, which have the following chemical formulas (**Figures 1** and **2**) [9]:

Recent reference studies indicate the use of turmeric root extract in 2012 to inhibit copper metal. The inhibit corrosion was 98% with EIS technology and Tafel polarization [10]. In 2014, the effect of turmeric on steel was studied with Tafel polarization in a petroleum medium. The inhibit corrosion was 92% [11]. In 2017,
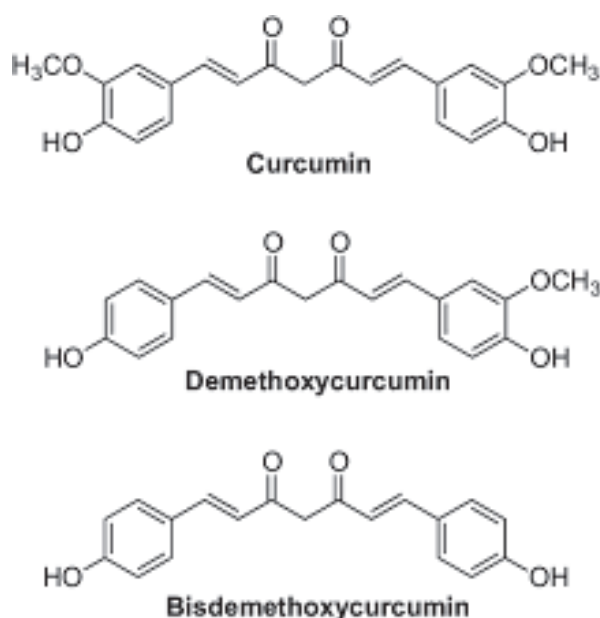

Figure 1.
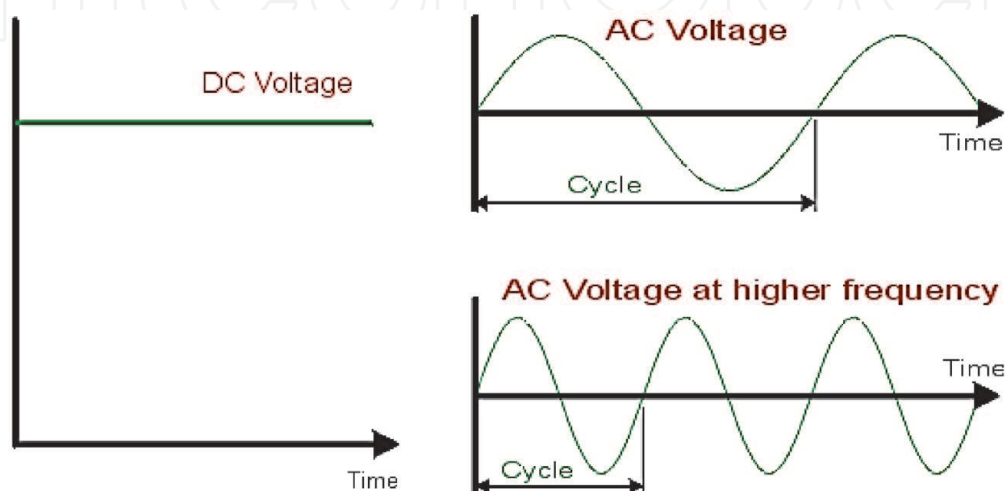*Chemical formulas for turmeric derivative compounds [9].*

Figure 2.
Sinusoidal signal applied and the sinusoidal current signal produced by a specific phase difference.

the effect of turmeric on solid carbon in a saline medium (3.5% NaCl) was studied with Tafel technology; the inhibit corrosion was 91% [12].

This phenomenon has not been adequately studied in Syria; therefore, this research is an important step in studying the phenomenon of corrosion and understanding the mechanism of its occurrence and the conditions affecting it with the latest technologies Electrochemical impedance spectrometry and Mott-Schottky plot are used as a basis for future research in order to implement solutions on the ground.

1.1 Definition of electrochemical impedance spectrometry (EIS)

Electrochemical impedance spectrometry is also called alternating current (AC) and impedance spectroscopy (EI). It is a useful tool and the newest method in many studies, especially the study of corrosion of minerals. Impedance is defined as the measurement of the impedance of alternating current passage in each part of the electrical circuit, and it has units of ohm. Electromagnetic impedance spectroscopy measures the sinusoidal changes of the current and potential signals as a function of the frequency at the value of a current, a field of current, a value of a potential, or a field of potential. Frequency changes give rise to a different phase difference between the current and potential signals for each circuit element [1].

Impedance is measured by applying a sinusoidal signal or current and then measuring the resulting response to the corresponding variable in a given frequency range. The following equations show the signal of latency and current response at a specific frequency [3], which are found via Eq. (1):

$$E_t = E_0 \sin (\omega t) \tag{1}$$

where E_t is the latency at time t, E_0 is the applied signal amplitude, ω is the angular frequency (radians/second) equal to $2\pi f$, and f (frequency) is the number of integrated vibrations per second (Hz/s).

The resulting current response is measured at the same frequency value with a phase difference between the current and potential signals and a difference in signal amplitude, which are found via Eq. (2):

$$I_t = I_0 \sin (\omega t + \varphi) \tag{2}$$

where φ is the phase difference in radians and I0 is the signal response amplitude. The relationship of impedance is given according to Ohm's law:

$$Z = E_t/I_t = E_0 (\sin (\omega t)/I_0 \sin (\omega t + \varphi)) \tag{3}$$

$$= Z_0 (\sin (\omega t)/ \sin (\omega t + \varphi)) \tag{4}$$

where $Z_0 = E_0/I_0$.

The value of the phase difference at the value of a specific frequency is given by

$$\tan \varphi = Z_{img}/Z_{real} \tag{5}$$

where Z_{img} is the imaginary impedance and Z_{real} is the true impedance.

1.2 Features and applications

The electromagnetic impedance spectroscopy is distinguished as its results are accurate, as each point of the EIS curve contains information about the electrical

process taking place, compared to conventional electrical methods that depend on measuring current changes, electrical charges, or the potential of the electrodes as a function of time, which depends on a certain value of its spectrum, such as a cyclic voltage, which includes current changes in hundreds of points for the potential to obtain a specific value for the peak oxidation and return at the corresponding current and potential value [3].

Among the applications of electromagnetic impedance spectroscopy, in addition to studying corrosion processes, electroplating processes, and semiconductors, it studies surface processes that include oxidation and reduction processes on the electrode surface, adsorption processes, electrical adsorption, and diffusion, as well as the kinetics of reactions in solutions, mass transfer, and resistance to solution, cells, and their electrical properties and batteries, determining the effect of each circuit element on impedance [1, 6]. It is also distinguished by not destroying the studied sample after testing [13].

2. Materials and methods

2.1 Preparation of plant extract

Turmeric root extract was prepared by washing and drying the turmeric root and grinding it then dissolving 1 g of powder in 100 mL methanol 50% and removing the solvent by placing the solution in a vacuum evaporator, at 60°C. Distilled water is used in the preparation process [14].

2.2 Preparation of metal specimen

The iron specimens have a composition (wt%) of 0.200% C, 0.500% Si, 1.600% Mn, 0.035% S, 0.035% P, 0.040% Nb, 0.012% N, 0.020% Al, and remaining Fe. This sample was analyzed in the Atomic Energy Commission and abraded with a series of emery papers 400, 1200, 1500, and 1800 grades. The samples were then washed thoroughly with distilled water and dried in air.

2.3 Test solution

A solution of 0.5 M concentrated acid was prepared using distilled water and 37% hydrochloric acid.

2.4 Electrochemical measurements

Electrochemical measurements were carried out using a potentiostat IVIUM-STAT.XR (Holland). A three-electrode cell system containing working electrode (iron coupon) of a 1 cm^2 exposed area, saturated (Ag/AgCl) electrode as a reference electrode, and then a platinum wire as auxiliary electrode was used. The electrochemical impedance spectroscopy measurements were carried out using the mentioned electrochemical system. Polarization curves were recorded at a sweep rate of 50 mV s^{-1}. Electrochemical impedance spectroscopy measurements were carried out at open-circuit potential over a frequency range of 1 MHz to 1 Hz. The sinusoidal perturbation has an amplitude of 0.01 mV.

2.5 Scanning electron microscopy (SEM) and energy dispersive X-rays (EDX)

The inhibitor film formation of the extracts surface was studied using SEM and EDX techniques.

3. Results and discussion

3.1 Mechanism of inhibition process

Turmeric root extract (TRE) used here as a corrosion inhibitor can serve as a scale inhibitor as well. This plant is characterized by the existence of a percentage of phenolic compounds (categories of curcumin) of a percentage up to 90%. It is a natural, nontoxic, environmentally friendly material. Active compounds in turmeric root extract are attributed to curcumin, demethoxycurcumin, and bisdemethoxycurcumin and to the multiple lone pair of electrons, multiple bonds, and/or conjugated л-type bond system [15]. Adsorption of these active molecules forms thin inhibitor films on the metal surface, which isolate the metal surface from the corrosive environment [16]. The oxygen atoms, the aromatic rings, and the bilateral bond of the aromatic rings boost the electronic pair freedom on the surface of the electrode. These compounds adsorb their free electrons on the surface of the electrode, and the iron is oxidized to form positively charged iron, thus forming a double electrical layer, and difference in voltage arises, as schematically presented in **Figure 3**. The inhibitor enhances the free electrons, which reduces iron corrosion and enhances inhibition.

3.2 Electrochemical impedance spectroscopy measurements

In the corrosion behavior of iron in 0.5 M HCl solution, in the absence and presence of TRE, it is investigated by the EIS, at 298 K after 1 hour of immersion in the acid solution. The double-layer capacitance (C_{dl}) and the frequency at which the imaginary component of the impedance is maximum ($-Z_{max}$) are found via Eq. (6):

$$C_{dl} = 1/w_{max}R_{ct} \text{ where } w_{max} = 2\pi f_{max} \qquad (6)$$

The inhibition efficiency $\%IE_{Rct}$ that resulted from the charge transfer resistance (R_{ct}) is calculated by

$$\%IE_{Rct} = \left[(R_{ct} - R^0{}_{ct})/R_{ct} \right] * 100 \qquad (7)$$
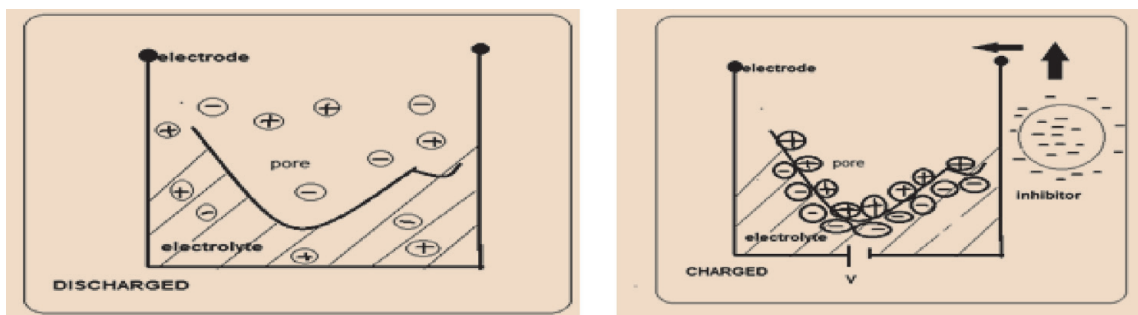

Figure 3.
Schematic presentation of the electric double-layer formation [Chem draw].

where R^0_{ct} and R_{ct} are the charge transfer resistance (R_{ct}) in the absence and presence of different concentrations of inhibitor, respectively [17].

Nyquist's and Bode's graphs of the results of the EIS of iron in 0.5 M HCl, in the absence and presence of different concentrations of TRE, were presented in **Figures 4** and **5**, respectively. The big capacitive loop refers to the adsorption of the inhibitor molecules (active compounds) presented in **Figure 2** on the iron samples [18]. R_s represents the resistance of the corrosive solution, and R_{ct} represents the effective resistance of the transport groups of the damper and the adsorption of their electrons onto the metal surface. C_{dl} is the amplitude of the formed double layer between the surface of the metal and solution.

Table 1 indicates that the R_{ct} values of the inhibited substrates increased with the concentration of inhibitors and C_{dl} values decreased because of the increased prevalence of active compounds from the inhibitor and the adsorption of their electrons on the iron surface, which confirms that TRE extract is an effective inhibitor of corrosion of iron in the medium of water chlorine acid [19]. The values of n between 0.7 and 0.98 indicate that the constant phase element Q operates as a capacitance in the equivalent electrical circuit, which indicates a complex. The adsorbent inhibitor is a capacitive capacitor in the electrical circuit equivalent to its positive bus, the surface of the solution, and the negative capacitor, the electrode surface [20]. Resistance values of the solution are small R_s due to the corrosion
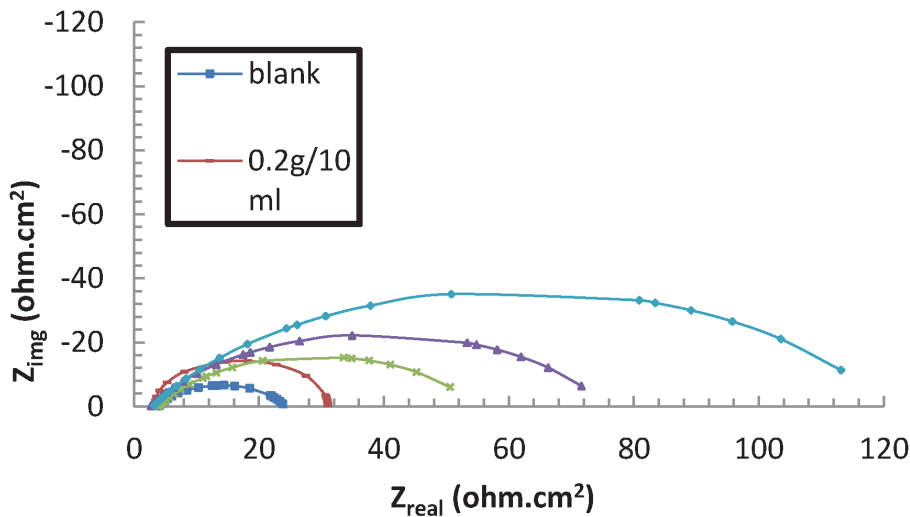

Figure 4.
Nyquist plots of iron in 0.5 M HCl containing varying concentrations of TRE after 1 hour of immersion in acid solution.
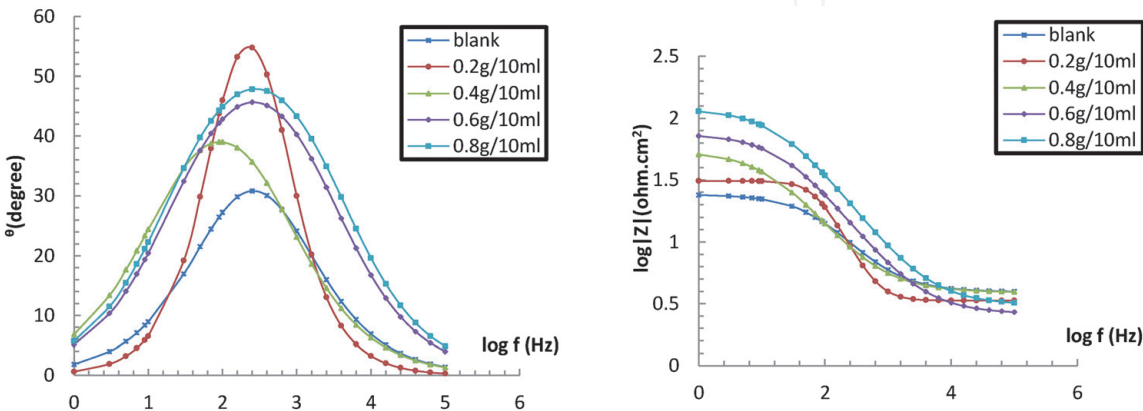

Figure 5.
Bode plots of iron in 0.5 M HCl containing varying concentrations of TRE after 1 hour of immersion in acid solution.

Inhibitor	Concentration (g/100 mL)	R_{ct} (ohm)	f_{max} (Hz)	C_{dl} (F/cm^2)	α	IE_{Rct}%
Blank	0.0	20.3	160	$4.90*10^{-5}$	0.73	—
Turmeric root extract	2.0	27.7	160	$3.59*10^{-5}$	0.98	26.71
	4.0	50.8	100	$3.13*10^{-5}$	0.70	60.04
	6.0	73.1	160	$1.36*10^{-5}$	0.70	72.23
	8.0	117	160	$8.51*10^{-6}$	0.70	82.65

Table 1.
Impedance parameters of corrosion of iron in 0.5 M HCl at 298 K in the absence and presence of different concentrations of TRE.
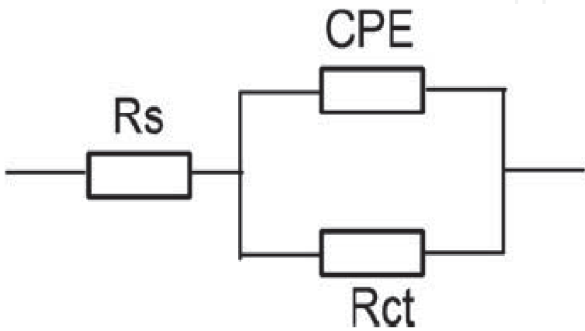

Figure 6.
Equivalent circuit model used to fit impedance spectra data.

Inhibitor	Concentration (g/100 mL)	E_{corr}- (mV/SCE)	I_{corr} (A*10^{-4}/cm^2)	βa (mV/dec)	βc (mV/dec)	CR (mm/year)	IE%
Blank	0.0	0.677	26.13	0.352	0.183	8.56	—
Turmeric root extract	2.0	0.3968	10.8	0.155	0.323	3.54	58.67
	4.0	0.474	4.7	0.146	0.233	1.55	82.01
	6.0	0.453	3.8	0.139	0.179	1.25	85.46
	8.0	0.417	3.4	0.131	0.225	1.11	86.99

Table 2.
Electrochemical parameters of iron in 0.5 M HCl solution at different concentrations without and with TRE.

concentration and temperature of the corrosive medium at different immersion times. Equivalent circuit model used to fit impedance spectra data is presented in **Figure 6**.

3.3 Potentiodynamic polarization measurements

3.3.1 Influence of concentration

Polarization measurements were done in order to know about the kinetics of the cathodic and anodic reactions. The anodic and cathodic current potential curves are extrapolated up to their intersection at a point where corrosion current density (I_{corr}) and corrosion potential (E_{corr}) are acquired [21]. **Table 2** shows the electrochemical parameters (I_{corr}, E_{corr}, βa, βc, and CR) obtained from Tafel plots for the iron electrode in 0.5 M HCl solution without and with various concentrations of

TRE. The I_{corr} values were used to calculate the inhibition efficiency, IE (%), in **Table 2**, using Eq. (8):

$$IE = [I - I_{corr}/I] * 100 \qquad (8)$$

where I_{corr} and I are the corrosion current densities with the presence and absence of inhibitor, respectively. The CR values in **Table 2** used the following equation [22]:

$$CR = 3.27 * 10^{-3} \, i_{corr} \, E_w/d \qquad (9)$$

where i_{corr} is the corrosion current density in micro A/cm^2, E_w is the equivalent weight of the corroding metal in grams, and d is the density of the corroding metal in g/cm^3.

Under the experimental conditions performed, the cathodic section of the plot represents the hydrogen evolution reaction, while the anodic section represents the iron dissolution reaction. They are determined by the extrapolation of Tafel lines to the respective corrosion potentials.

The results in **Table 3** indicates that the inhibitor reduces the corrosion current value and inhibition; IE (%) increases with the concentration of the inhibitor reaching 88. 90%, at 8 g/100 mL. This result suggests that good inhibition act for TRE [23].

T (K)	C (g/100 mL)	E$_{corr}$- (mv/SCE)	I$_{corr}$ (μA/cm^2)	βa (mV/dec)	βc (mV/dec)	CR mm/year	IE%
283	Blank	0.677	26.13	0.352	0.183	8.56	—
	2	0.3968	10.8	0.155	0.323	3.54	58.67
	4	0.468	5.9	0.148	0.177	1.933	77.42
	6	0.453	3.8	0.139	0.179	1.25	85.46
	8	0.442	2.9	0.143	0.188	0.979	88.90
293	Blank	0.661	31.1	0.316	0.174	10.19	—
	2	0.379	8.35	0.142	0.328	2.73	73.15
	4	0.458	6.6	0.138	0.205	2.167	78.78
	6	0.458	4.8	0.164	0.206	1.581	84.57
	8	0.441	4	0.131	0.193	1.318	87.14
303	Blank	0.677	33.8	0.331	0.168	11.07	—
	2	0.452	13.5	0.167	0.249	4.4	60.06
	4	0.426	9	0.132	0.263	2.97	73.37
	6	0.474	7	0.152	0.193	2.29	79.29
	8	0.498	5.7	0.14	0.16	1.87	83.14
313	Blank	0.714	36.2	0.378	0.119	11.84	—
	2	0.477	14.6	0.188	0.237	4.788	59.67
	4	0.419	11	0.135	0.28	3.631	69.61
	6	0.379	7.9	0.133	0.339	2.6	78.18
	8	0.468	5.9	0.148	0.177	1.933	83.70

Table 3.
Polarization parameters of iron in 0.5 M HCl at different temperatures with various concentrations of TRE.

3.3.2 Influence of temperature

Polarization curves for the iron in 0.5 M HCl solution are shown in **Figures 7** and **8** in two different conditions, with constant concentrations of TRE and in the presence of different concentrations of TRE in the temperature range 283–313 K. The surface overage (Θ) was calculated using

$$\Theta = \text{IE (\%)}/100 \tag{10}$$

The inhibition efficiency IE (%) is given by Eq. (8).

The results of the **Table 2** refer that temperature increase leads to I_{corr} increase, while the addition of TRE resulted in the decrease of the I_{corr} values across the temperature range. The results also indicate that the inhibition efficiencies increased with the concentration of inhibitor but decreased proportionally with temperature. Such behavior can be rationalized that the inhibitor acts by adsorption onto the metal surface [24].
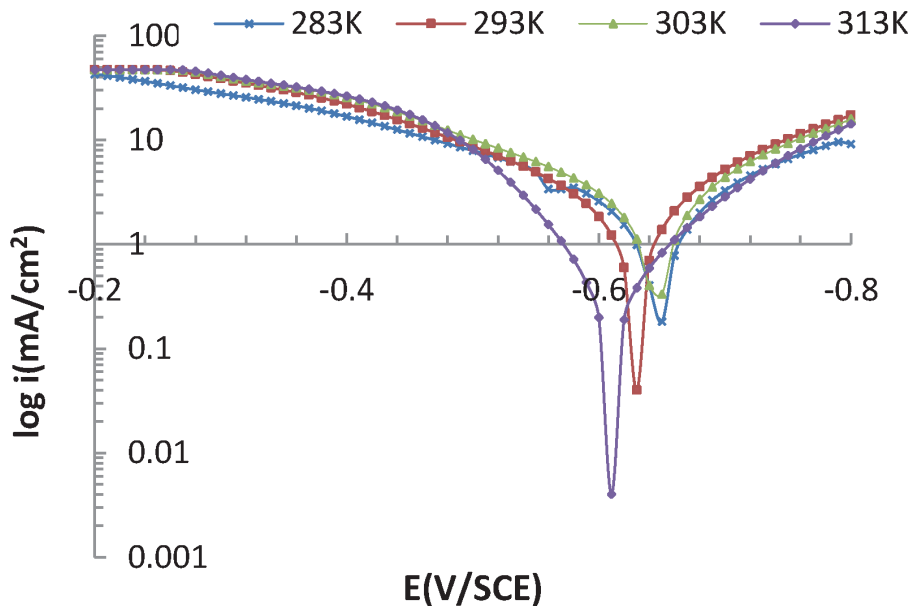

Figure 7.
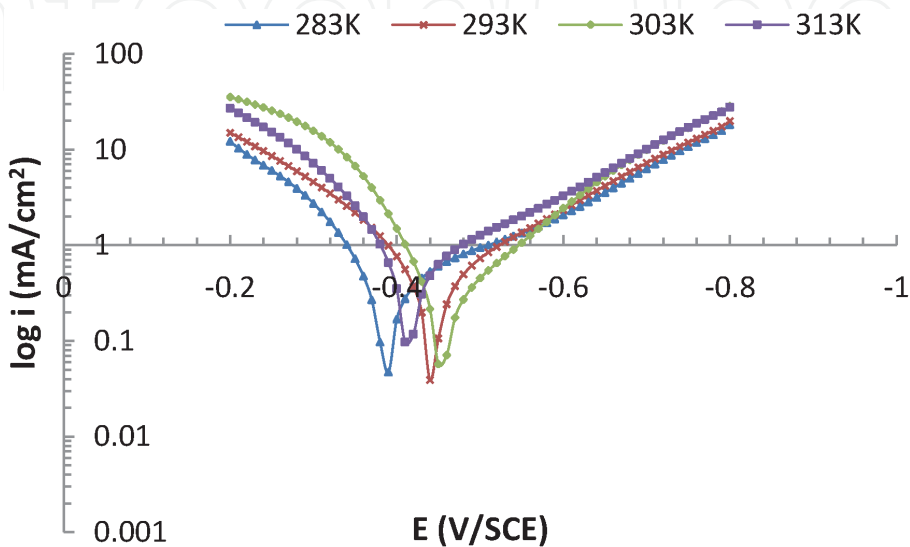*Polarization curves of iron in 0.5 M HCl at different temperatures.*

Figure 8.
Polarization curves of iron in 0.5 M HCl at different temperatures in the presence of 8 g/100 mL of TRE.

Ea, ΔS*, and ΔH*, for both corrosion inhibition and corrosion of iron in 0.5 M HCl in the presence and absence of TRE at different concentrations between 283 and 313 K, were calculated from an Arrhenius-type plot (Eqs. (11) and (12)) [25]:

$$\text{Log } (I_{corr}) = -E_a/2.303RT \tag{11}$$

where I_{corr} is the corrosion current density (taken from averaged polarization), Ea is the activation of ion energy, and R is the universal gas constant.

$$I = \frac{RT}{Nh} \exp\left(\frac{\Delta S*}{R}\right) \exp\left(-\frac{\Delta H*}{RT}\right) \tag{12}$$

where h is Plank's constant, N is Avogadro's number, ΔH^*_a is the enthalpy of activation, and ΔS^*a is the entropy of activation.

The plots of Log (I_{corr}) vs. 1/T and Log (I_{corr}/T) vs. 1/T gave straight lines with the slope of -E_a/R and -ΔH* /R, respectively. The intercepts were A and [Ln (R/Nh) + (ΔS*/R)] for the Arrhenius and transition state equations, respectively (**Figures 9** and **10**). The calculated values of the activation energy Ea, the entropy of activation ΔS*, and the enthalpy of activation ΔH* are presented in **Table 4**.

The activation energy values with TRE film are greater than the absence as shown in **Table 4**. This result is consistent with previous results, since adsorption of active compounds on the metal surface impeded the corrosion reaction as if an additional energy barrier had arisen to dampen the corrosion reaction. The positive signal for a change in the enthalpy of the corrosion reaction indicates that the
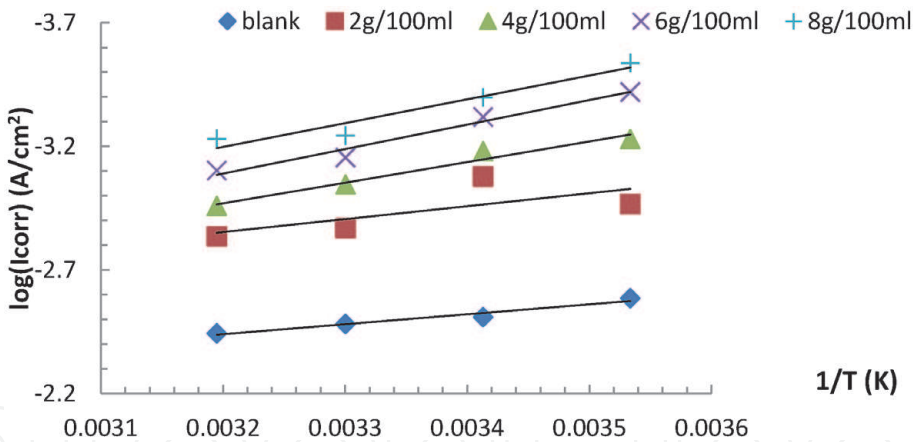

Figure 9.
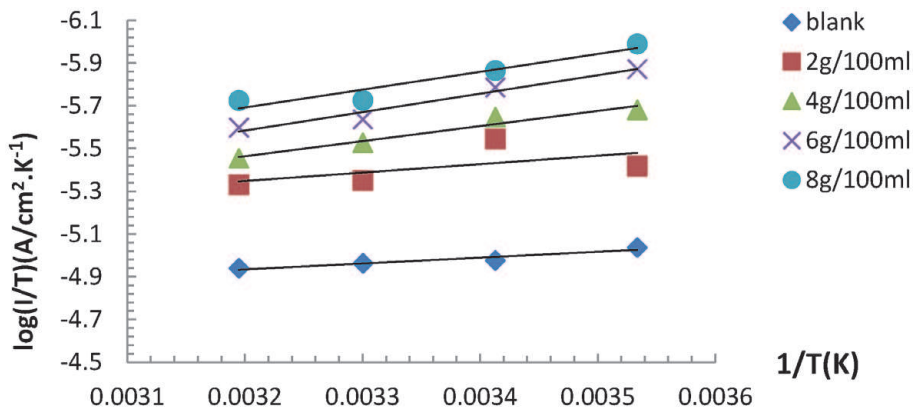*Arrhenius plots of log (I_{corr}) versus 1/T at various concentrations of TRE.*

Figure 10.
Variation of log (I_{corr}/T) versus 1/T at various concentrations of TRE.

Inhibitor	C (g/100 mL)	Ea (kJ/mol)	ΔH* (kJ/mol)	ΔS* (J/mol)
0.5 M HCl	—	7.69	5.22	−275.37
Turmeric root extract (TRE)	2.0	10.02	7.55	−275.83
	4.0	15.99	13.52	258.93
	6.0	18.99	16.52	−251.65
	8.0	18.43	15.96	−255.51

Table 4.
Values of activation parameters ΔS and ΔH* for iron 0.5MHCl in the presence and absence of various inhibition concentrations.*
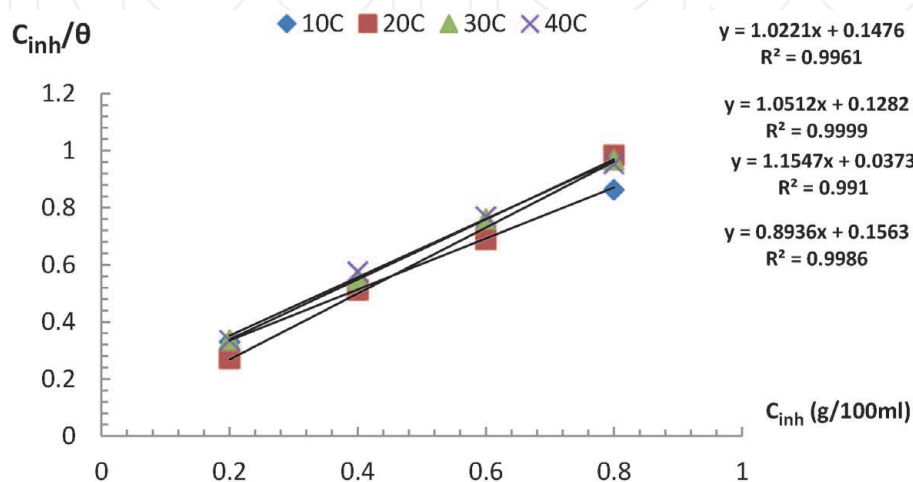

Figure 11.
Plots of Langmuir adsorption isotherm of TRE on iron surface at different temperatures.

pyrolysis process is endothermic. The decreasing entropy of the reaction at the formation of the complex indicates that the adsorbent inhibitor complex has a coherent structure [26–28].

The study of adsorption behavior of active compounds on the iron surface shows the following data:

3.3.3 Adsorption isotherm

Study the effect of turmeric root extract concentration on the inhibition efficacy by acting C\θ in terms of C. Gibbs standard free energy (ΔG_{ads}) is calculated as a single molecule of water, which replaces a molecule. One of the inhibitor molecules has a ratio of 1/55.5, from relationships (13) and (14), according to the isotope of the immersion in adsorption. Langmuir adsorption isotherm is represented by Eq. (13) [29]:

$$\text{Log K} = \log (1\backslash 55.5) - \Delta G^0_{ads}\backslash RT \qquad (13)$$

Rearrangement gives Eq. (14):

$$C\backslash \theta = 1/K_{ads} + C \qquad (14)$$

where θ is the degree of surface cover with the inhibitor, K_{ads} is the adsorption equilibrium constant, and C is the concentration of inhibitor used in the corrosive medium (**Figure 11**).

T (K)	1/K	ΔG_{ads} (kJ mol^{-1})	ΔSa (J mol^{-1})	R^2	ΔHa (kJ mol^{-1})
283	0.16	−13.8169	48.75	0.9986	−20
293	0.04	−17.7954	60.67	0.9910	
303	0.13	−15.2926	50.40	0.9999	
313	0.15	−15.4306	49.24	0.9961	

Table 5.
Calculated parameters of Langmuir adsorption isotherm.
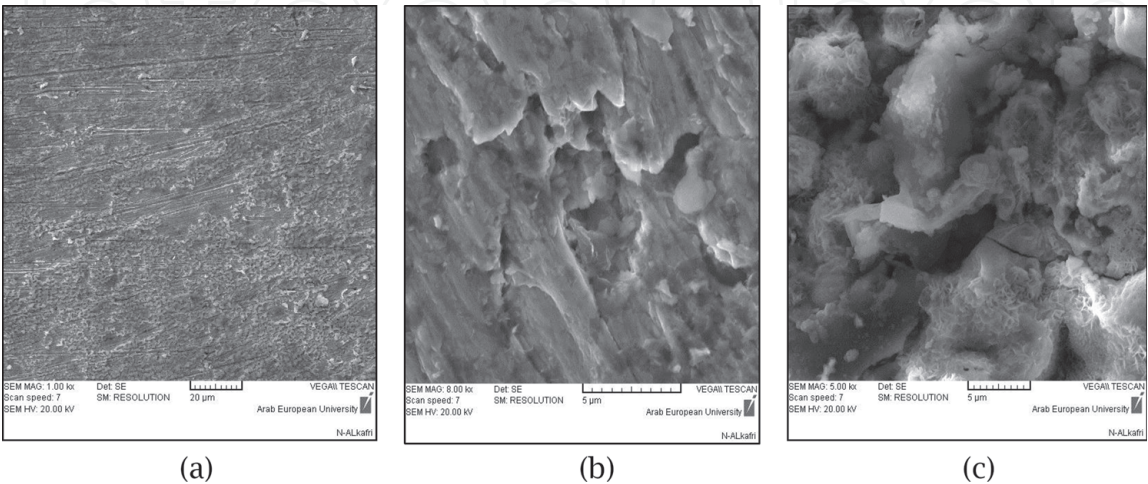

(a)   (b)   (c)

Figure 12.
SEM of polished iron (a) before immersion (b) after 1 hour of immersion in HCl 1 g/100 mL of TRE and (c) treated iron in the presence of 1 g/100 mL extract.

The value of ΔG_a is less than −20 kJ mol^{-1} which is an indication that physical adsorption is dominant [30] (**Table 5**).

3.4 SEM–EDX analysis

Surface morphology of iron was studied by scanning electron microscopy after 1 h immersion in HCl with and without addition of the inhibitor. **Figure 12a** represents the micrograph obtained by polished steel before exposing to the corrosive medium, while **Figure 12b** showed strongly damaged steel surface due to the corrosion effect after immersion in HCl solution. SEM images of steel surface after 1 hour immersion in HCl with 1 g/100 mL TRE are shown in **Figure 12c**. It can be seen from **Figure 12a** that the iron sample before immersion seems smooth and shows some abrading scratches on the surface. Inspection of **Figure 12b** reveals that the iron surface after immersion in uninhibited HCl shows an aggressive attack of the corroding medium on the iron surface. In contrast, in the presence of 1 g/100 mL TRE (**Figure 12c**), the iron surface was corroded only negligibly. In addition, there was an adsorbed film on the iron surface that was not observed in **Figure 12b**. These results confirmed enhancement of surface coverage of steel surface that led to

Element	C	O	Cl
Without inhibitor	0.20	—	—
After adding HCl	0.20	29.86	1.76
With inhibitor	26.84	7.14	0.1

Table 6.
The percentages of the studied elements in the presence of TRE.

the decrease in contact between the iron and the aggressive medium. Thus, a good adsorptive protection layer that was formed by the inhibitor can efficiently inhibit corrosion of steel.

The following table shows the percentages of the studied elements in the presence and absence of TRE.
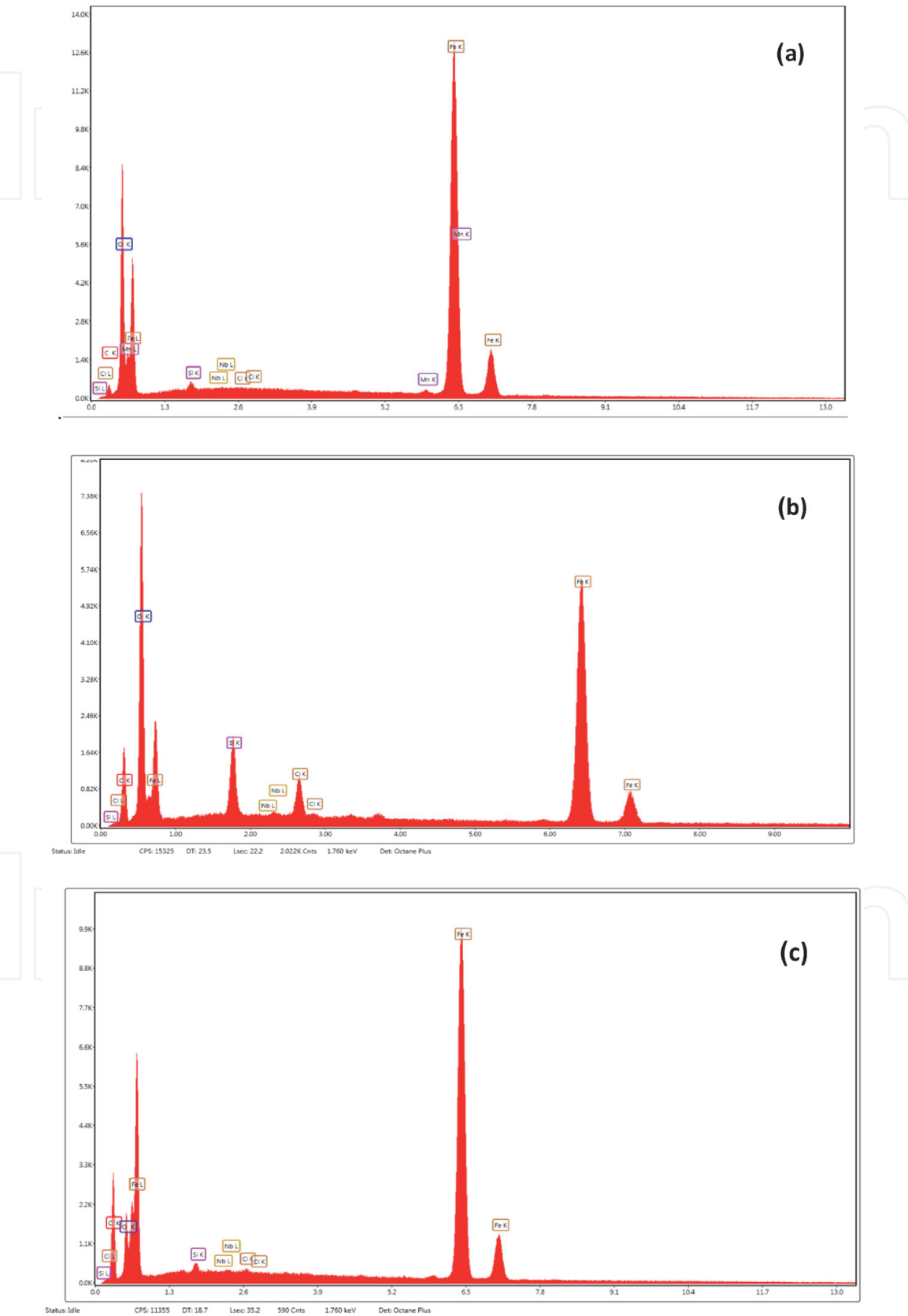

Figure 13.
EDX of (a) polished iron, (b) after 1 hour of immersion in HCl, and (c) treated iron in the presence of 1 g/ 100 mL extract.

Increasing the percentage of carbon on the surface of the iron treated with the inhibitor compared to the surface of the polished iron is presented in **Table 6** and **Figure 13**, due to the spread of the effective groups in the inhibitor and the adsorption of its electrons on the surface of the iron. Oxygen content is reduced at the surface of the iron treated with an inhibitor, compared to the surface of iron exposed to the corrosive medium, due to its interaction with iron to form a complex inhibitor film. Chlorine content is reduced in the presence of the extract compared to the iron surface exposed to corrosive medium due to the reaction of chlorine with iron forming chloride dissolved iron.

4. Conclusion

The inhibition efficiency (%IE) of TRE increases with the increase of extract concentration. EIS results showed that the double-layer capacitance (Cdl) decreases and charge transfer resistance (Rct) increases with the time of immersion in the extract. The inhibitor showed maximum inhibition efficiency (%IE), 88.9% at 8 g/100 mL concentration. The inhibition efficiency (%IE) of TRE decreased with temperature, which leads to a decrease in activation energy (E_a) of the corrosion process.

The activation energy value of $E_a = -20$ kJ mol^{-1} indicates that the adsorption process is spontaneous and the is physical adsorption. Langmuir adsorption isotherm and SEM studies showed that TRE inhibitions occur through adsorption mechanism. The results of SEM and EDX have been shown to form a protective film on the iron surface.

Acknowledgment

Author details

Khuloud Almzarzie*, Ayman Almassri, Ahmad Falah and Hassan Kellawi
Department of Chemistry, Damascus University, Syria

*Address all correspondence to: kholod.m990@gmail.com

IntechOpen

References

[1] Ahmed A, Kadhum AH, Abdulhadi K. Inhibition of mild steel corrosion in sulfuric acid solution by new Schiff Base. In: Process Engineering. Vol. 7. Malaysia: University Kebangsaan; 2014. pp. 787-804

[2] Ferreira ES, Giacomelli C, Giconelli FC, Spinelli A. Evaluation of the inhibitor effect of L-ascorbic acid on the corrosion of mild steel. Materials Chemistry and Physics. 2004;**83**:129-134

[3] Bentiss F, Gassama F, Barbry D, Gengembre L, Vezin H, Lagrenée M, et al. Corrosion inhibition of mild steel in acidic media using newly synthesized heterocyclic organic molecules: Correlation between inhibition efficiency and chemical structure. Applied Surface Science. 2006;**252**

[4] Lagrenee M, Mernari B, Chaibi N, Traisnel M, Vezin H, Bentiss F. Corrosion inhibition of mild steel in acidic media using newly synthesized heterocyclic organic molecules: Correlation between inhibition efficiency and chemical structure. Corrosion Science. 2001;**43**

[5] Ayers RC, Hackerman N Jr. Corrosion inhibition in HCl using methyl pyridines. Journal of the Electrochemical Society. 1963;**110**(6):507-513

[6] Moretti G, Guidi F, Grion G. Tryptamine as a green iron corrosion inhibitor in 0.5M deaerated sulphuric acid. Corrosion Science. 2004;**46**(2):387-403

[7] Quraishi MA, Rawat J, Ajamal M. Dithiobiurets: A novel class of acid corrosion inhibitors for mild steel. Journal of Applied Electrochemistry. 2000;**30**(6):745-751

[8] Khalil N. Quantum chemical approach of corrosion inhibition. Electrochimica Acta. 2003;**48**:2635-2640

[9] Kairi N. The Effect of Temperature on the Corrosion Inhibition of Mild Steel in 1 M HCl Solution by *Curcuma longa* Extract. Malaysia: Universiti Sains; 2013. pp. 7138-7155

[10] Jinendra G. Corrosion Inhibition by Turmeric Extract. India: RGPV University; 2012. pp. 10455-10458

[11] Aprael S et al. Corrosion Inhibition of Mild Steel by Curcuma Extract in Petroleum Refinery Wastewater. Iraq: University of Baghdad; 2014

[12] Saleh K et al. Inhibition and Adsorption Actions of Nano Curcumin for Corrosion of Carbon Steel Alloy in 3.5% NaCl Solution. Baghdad, Iraq: University of Baghdad, Collage of Science; 2017. pp. 515-529

[13] Johnsirani V et al. Curcumin dye as corrosion inhibitor for carbon steel in sea water. Chemical Science Transactions. 2013

[14] Benali O, Larabi L, Traisnel M, Gengembra L, Harek Y. Study on the inhibition of mild steel corrosion by quaternary ammonium compound in H2SO4. Applied Surface Science. 2007;**253**:6130

[15] Abdel-Gaber AM, Hijazia KM, Younesa GO, Nsouli B. Comparative study of the inhibitive action between the bitter orange leaf extract and its chemical constituent linalool on the mild steel corrosion in HCl solution. Química Nova. 2017;**230**

[16] Mohamed HA, Farag AA, Badran BM. Corrosion Inhibition of Mild Steel Using Emulsified Thiazole

Adduct in Different Binder Systems. Vol. 10. Cairo, Egypt: Department of Polymers and Pigments, National Research Center; 2008. pp. 67-77

[17] Abdel Hamid Z. Clarification of the corrosion inhibition of mild steel in hydrochloric acid solutions via Cetyltrimethyl ammonium bromide inhibitor. Egyptian Journal of Chemistry. 2014;**57**(5):353-371

[18] Shukla SK, Quraishi MA. The effects of pharmaceutically active compound doxycycline on the corrosion of mild steel in hydrochloric acid solution (HCl). Corrosion Science. 2010;**52**:314

[19] Yurt A, Balaban A, Kandemir SU, Bereket G, Erk B. Adsorption and corrosion inhibition characteristics of some nicotinamide derivatives on mild steel in hydrochloric acid solution (HCl). Materials Chemistry and Physics. 2004;**85**

[20] Hui Cang W. Study of Stevia rebaudiana Leaves as Green Corrosion Inhibitor for Mild Steel in Sulphuric Acid by Electrochemical Techniques. College of chemical engineering and biological, Yancheng institute of technology; 2012. pp. 3726-3736

[21] Abd EI-Rehim S, Ibrahim MAM, Khaled KF. 4-Aminoantipyrine as an inhibitor of mild steel corrosion in HCl solution. Journal of Applied Electrochemistry. 1999;**29**

[22] Ch W-M, Post F, Joshua L, Sazzadur R, Anjali T. Sub-Surface Corrosion Research on Rock Bolt System, Perforated SS Sheets and Steel Sets for the Yucca Mountain Repository. Vol. 302004

[23] Bentiss F, Bouanis M, Mernari B, Traisnel M, Vezin H, Lagrenee M. Applied Surface Science. 2007;**253**

[24] Noor EA, Al-Moubaraki AH. Thermodynamic study of metal

corrosion and inhibitor adsorption processes in mild steel/1-methyl-4[4′ (−X)-styryl] pyridinium iodides/ hydrochloric acid systems. Materials Chemistry and Physics. 2008;**110**

[25] Sayyah SM, Abd El-Rehim MM, Mohamed SM. Corrosion inhibition of Aluminium with a series of aniline monomeric surfactant and their analogues polymers in 0.5 M HCl solution. Egyptian Journal of Chemistry. 2012;**55**(6):583-602

[26] Maqsood AM, Ali H, Firdosa N, Shaeel A, Zaheer K. Anti-corrosion ability of surfactants. International Journal of Electrochemical Science. 2011;**6**:1927-1948

[27] Abd El-Rahim SS, Refaey SAM, Taha F, Saleh MB, Ahmed RAJ. Novel cationic surfactants from fatty acids and their corrosion inhibition efficiency for carbon steel pipelines in 1 M HCl. Journal of Applied Electrochemistry. 2001;**31**

[28] Abd El-Rehim SS, Hassan HH, Amin MA. Corrosion inhibition of aluminum in hydrochloric acid solution (HCl) using potassium iodate inhibitor. Materials Chemistry and Physics. 2001;**70**

[29] Bilgic S, Caliskan N. Inhibition of steel corrosion in hydrochloric acid solution (HCl) by chamomile extract. Applied Surface Science. 1999;**152**

[30] Tsuru T, Haruyama S, Gijutsu B. Corrosion monitor based on impedance method; construction and its application to homogeneous corrosion. Japan Society of Corrosion Engineering. 1978;**27**